Adaptive Transmit Power Control in IEEE 802.11a Wireless LANs

Daji Qiao[+]   Sunghyun Choi[*]   Amit Jain[+]   Kang G. Shin[+]
[+]The University of Michigan   [*]Seoul National University
Ann Arbor, MI 48109, USA   Seoul, 151-742, Korea
{dqiao,amitj,kgshin}@eecs.umich.edu   schoi@snu.ac.kr

Abstract—Transmit power control (TPC) has been recognized as one of the effective ways to save energy in wireless devices. In this paper, we demonstrate the energy-efficient Distributed Coordination Function (DCF) operation of IEEE 802.11a wireless LANs (WLANs) via TPC and physical layer (PHY) rate adaptation. The key idea is to enforce an RTS/CTS frame exchange before each data transmission, and then select the most energy-efficient combination of the PHY mode and the transmit power level for the subsequent data frame transmission to save energy. The performance of the proposed scheme is evaluated via simulation in the ns-2 simulator.

I. INTRODUCTION

In wireless local-area networks (WLANs), most wireless devices such as laptops and palmtops are battery-powered, and extending the operating time of such devices is always desirable and important. A WLAN device normally operates in one of the following modes: *transmit mode*, *receive mode*, or *sleeping mode*. Applying transmit power control (TPC) in WLAN systems, which allows a WLAN device to use one of the available power levels in transmit mode, is naturally an attractive idea to save battery energy and has been receiving considerable attention.

A. Problem Statement

IEEE 802.11 [1] specifies two different medium access control (MAC) mechanisms in WLANs: the contention-based Distributed Coordination Function (DCF) and the polling-based Point Coordination Function (PCF). IEEE 802.11a physical layer (PHY) [2] is the new high-speed PHY developed to operate 802.11 in the 5 GHz Unlicensed National Information Infrastructure (U-NII) band, which provides 8 PHY modes with transmission rates from 6 Mbps up to 54 Mbps. In [3], we derived the energy consumption performance analytically for uplink data transmissions in an IEEE 802.11a WLAN under the PCF, and demonstrated the energy-efficient PCF operation via both TPC and PHY rate adaptation. In this paper, we address another closely-related but more difficult problem: how to apply TPC to save energy under the DCF? The WLAN architecture we are interested in is an infrastructure basic service set (BSS).

BSS is the basic building block of an IEEE 802.11 WLAN. It consists of a set of stations controlled by a single coordination function. There are two types of BSS [4]: independent BSS and infrastructure BSS. The infrastructure BSS includes an access point (AP) and is the most widely-deployed WLAN architecture. For this reason, we focus on the energy-efficient DCF operation in an infrastructure BSS. Moreover, since the AP is normally located at a fixed position and connected to the power line, energy consumption at the AP for downlink (AP-to-station) transmissions is usually not

a critical issue. We are more concerned about energy savings at battery-operated wireless stations for uplink (station-to-AP) transmissions.

In an infrastructure BSS, if a wireless station wants to communicate with another station, the frames must be first sent to the AP, and then from the AP to the destination. Due to this reason, all the wireless stations must be able to hear the AP, but they are not required to hear each other, and thus, they may appear hidden to each other. Moreover, as described in [5], by simply allowing wireless stations to transmit at different power levels under the DCF, the number of hidden terminals is likely to increase, which, in turn, results in more collisions and re-transmissions due to the very nature of DCF's contention-based access mechanism, and hence, more energy is consumed eventually. Recognizing the above "hidden nodes" problem under the DCF, we propose a novel way to exercise TPC under the DCF. The key ideas are that (1) an RTS/CTS frame exchange is required before each data transmission; (2) the CTS frames are transmitted at the full power level by the AP to eliminate the hidden terminals; and (3) in order to deliver a data frame with minimum energy consumption, the most energy-efficient combination of the PHY mode and the transmit power level are adaptively selected for the next transmission attempt of the frame. Note that there is no such "hidden nodes" problem under the PCF since the access to the wireless medium is centrally-controlled by the AP, thus making the application of TPC to save energy under the PCF less hassle [3].

B. Related Work

In recent years, several power-management policies have been proposed to force a WLAN device to sleep adaptively at appropriate moments to save battery energy [6], [7], [8]. Since TPC determines the best transmit power level to use in transmit mode, our scheme is complementary to those power-management policies, which address how to switch between transmit/receive and sleeping modes.

In [9], the authors presented a Power-Aware Routing Optimization (PARO) scheme to achieve energy-efficient routing in multi-hop wireless networks. Similar to our scheme, the RTS/CTS frames are exchanged before the actual data transmissions, and they are transmitted at the full power level. On the other hand, the data and acknowledgment frames may be transmitted at lower power levels. Another similar power control scheme was presented in [10], where the transmit power levels of the data frames are dynamically adjusted with help of an enhanced RTS/CTS mechanism. The authors of [11] proposed to save energy in IEEE 802.11 WLAN devices by a combined tuning of the transmit power and the data frame size. None of the above schemes considers PHY rate adaptation. Since the 802.11 PHYs support multiple transmission rates, utilizing them adaptively by choosing the best PHY rate at a give time can enhance the system performance. Hence, PHY rate adaptation should be considered in conjunction with TPC.

433

C. Organization

The rest of this paper is organized as follows. Section II describes our proposed energy-efficient DCF operation and Section III presents and evaluates the simulation results. The paper concludes with Section IV.

II. THE ENERGY-EFFICIENT DCF OPERATION

In this section, we present the details of the energy-efficient DCF operation. The key idea is to combine TPC with adaptive PHY mode selection, so that the proper PHY rate as well as the best transmit power level can be adaptively selected for the next transmission attempt of a data frame, according to the up-to-date retry counts of the frame and the path loss condition, thus delivering data with minimum energy consumption. Besides, in order to avoid potentially more hidden terminals due to TPC, an RTS/CTS frame exchange is required prior to each data transmission.

A. The Enhanced Four-Way Frame Exchange

We illustrate how to enhance the four-way RTS-CTS-Data-Ack frame exchange to accommodate our idea, and why to do so, using a sequence of figures. In these figures, the dashed circle represents the coverage of the AP, i.e., the scope of the infrastructure BSS centered by the AP, and its radius is determined by assuming the nominal transmit power for the AP and the average background noise level. The conjunction area of the solid circle(s) is the area within which all the wireless stations are prevented from colliding with the on-going uplink data transmission from the transmitter (STA) to the AP. This is because these wireless stations can either update their NAVs after the RTS/CTS receptions or sense the wireless medium busy, and then defer their transmission attempts. The wireless stations outside this area are considered hidden to the transmitter.

Fig. 1(a) shows a simple two-way Data-Ack frame exchange when the data frame is transmitted using the nominal transmit power. Clearly, without RTS/CTS support, some wireless stations, e.g., w1 and w4, are hidden to the transmitter. Moreover, if we simply allow the transmitter to apply TPC on its data transmissions, the number of hidden terminals is likely to increase. As shown in Fig. 1(b), there is one more hidden terminal, w2, if the transmitter uses the minimum required transmit power to reach the AP for its data transmissions.
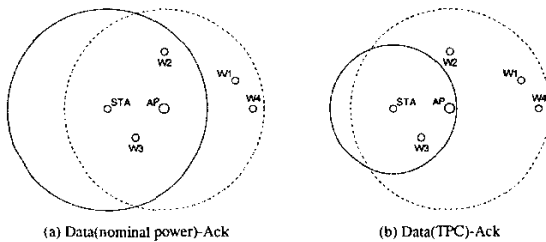

(a) Data(nominal power)-Ack   (b) Data(TPC)-Ack

Fig. 1. Two-way Data-Ack frame exchange

The RTS/CTS mechanism is one of the effective ways to alleviate the "hidden nodes" problem under the DCF. Fig. 2(a) shows a four-way RTS-CTS-Data-Ack frame exchange when the RTS/CTS frames are exchanged using the nominal transmit power. Since in an infrastructure BSS, all the wireless stations should be able to hear the AP, they can set their NAVs correctly upon reception of the CTS

frames and there are no more hidden terminals in the network. This scheme works well when the background noise level is stable and the user mobility is low. However, if the background noise level increases, the range within which a wireless station is able to correctly set the NAV shrinks, which, if combined with a high degree of user mobility, may result in the following three potential problems, as shown in Fig. 2(b). First, stations w1 and w4 become hidden terminals again. Second, if the transmitter moves to position I after its RTS transmission, it won't be able to receive the CTS frame from the AP correctly, and thus, the data transmission won't start at all. Third, if station w3 moves to position II after it receives the RTS frame from the transmitter but before receiving the CTS frame from the AP, then according to the 802.11 standard, w3 may reset its NAV, which was originally set according to the RTS reception. It is interesting to notice that all three problems are due to erroneous CTS receptions.

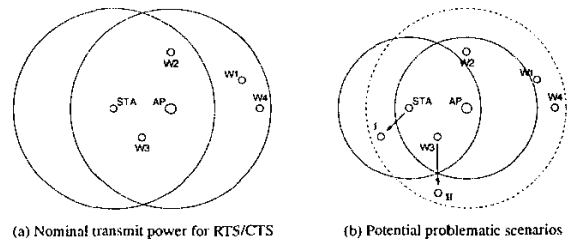(a) Nominal transmit power for RTS/CTS   (b) Potential problematic scenarios

Fig. 2. Four-way RTS-CTS-Data-Ack frame exchange

Based on the above observations, we propose to enhance the original four-way frame exchange to achieve the energy-efficient DCF operation as follows. First, the CTS frames are transmitted at the full power level to eliminate the hidden terminals. Second, the Ack frames are transmitted at the full power level as well to avoid the Ack transmission errors. One can do this because both CTS and Ack frames are transmitted by the AP, which is normally connected to the power line, and thus the energy consumption at the AP for downlink transmissions are not critically important. Third, the data frames are transmitted using the most appropriate combination of the PHY mode and the transmit power level, such that the energy consumption is minimized. Note that we need to select the mode-power combination for the data transmission attempt before the RTS frame is transmitted, so the duration information carried in the RTS frame can be properly set according to our PHY mode selection.

B. Pre-Built Mode-Power Combination Table

We solve the problem of finding the best mode-power combination $\{m^*, \mathcal{P}_t^*\}$ by applying the dynamic programming technique. A wireless station computes off-line the mode-power combination table indexed by the data payload length (ℓ), the path loss condition (s) from itself to the AP, and the frame retry counts (SRC, LRC). Each entry of the table is the best mode-power combination in the sense of minimizing the expected average energy consumption $(\mathcal{J})$ under the corresponding situation. Note that $\mathcal{J}$ is the ratio of the expected total energy consumption $(\mathcal{E})$ to the expected delivered data payload $(\mathcal{L})$, and is measured in *Joule per delivered data bit*. At run-time, the wireless station estimates s and selects the best mode-power combination for the next data frame transmission attempt by a simple table lookup. We assume that the transmission error (due to background noise) probabilities of the RTS, CTS, and Ack frames

are negligible because of their small frame sizes and robust transmission rates. The table entries are computed as follows.

First, consider the special case when SRC is equal to *dot11ShortRetryLimit* and/or LRC is equal to *dot11LongRetryLimit*. Obviously, since at least one of the frame retry limits has been reached, the data frame will be discarded without further transmission attempts. Hence, for any m and $\mathcal{P}_t$, we always have

$$\begin{cases} \mathcal{E}(m, \mathcal{P}_t, \ell, s, dot11ShortRetryLimit, \text{LRC}) = 0, \\ \mathcal{L}(m, \mathcal{P}_t, \ell, s, dot11ShortRetryLimit, \text{LRC}) = 0, \end{cases} \quad (1)$$

and

$$\begin{cases} \mathcal{E}(m, \mathcal{P}_t, \ell, s, \text{SRC}, dot11LongRetryLimit) = 0, \\ \mathcal{L}(m, \mathcal{P}_t, \ell, s, \text{SRC}, dot11LongRetryLimit) = 0. \end{cases} \quad (2)$$

Now, let's consider the general case when $0 \leq \text{SRC} < dot11ShortRetryLimit$ and $0 \leq \text{LRC} < dot11LongRetryLimit$. Assume that PHY mode m and transmit power $\mathcal{P}_t$ are selected for the next data transmission attempt. The frame delivery is successful only if the RTS transmission succeeds without collision and the data transmission is error-free or results in correctable errors. Otherwise, the station has to re-contend for the wireless medium to re-transmit the frame. Based on the above observations, we can construct the following recursive relations:

$$\mathcal{J}(m, \mathcal{P}_t, \ell, s, \text{SRC}, \text{LRC}) = \frac{\mathcal{E}(m, \mathcal{P}_t, \ell, s, \text{SRC}, \text{LRC})}{\mathcal{L}(m, \mathcal{P}_t, \ell, s, \text{SRC}, \text{LRC})}, \quad (3)$$

where

$$\begin{aligned}
&\mathcal{E}(m, \mathcal{P}_t, \ell, s, \text{SRC}, \text{LRC}) = \\
&\overline{\mathcal{E}}_{bkoff}(\text{SRC}, \text{LRC}) + \overline{\mathcal{E}}_{freeze} \\
&+ (1 - P_{c,rts}) \cdot [1 - P_{e,data}(m, \mathcal{P}_t, \ell, s)] \\
&\quad \cdot [\mathcal{E}_{rts-sifs-cts-sifs} + \mathcal{E}_{data}(m, \mathcal{P}_t, \ell) + \mathcal{E}_{sifs} \\
&\qquad + \mathcal{E}_{ack} + \mathcal{E}_{difs}] \\
&+ (1 - P_{c,rts}) \cdot P_{e,data}(m, \mathcal{P}_t, \ell, s) \\
&\quad \cdot [\mathcal{E}_{rts-sifs-cts-sifs} + \mathcal{E}_{data}(m, \mathcal{P}_t, \ell) + \mathcal{E}_{ack\_tout} \\
&\qquad + \mathcal{E}(m^*(\ell, s, \text{SRC}, \text{LRC+1}), \mathcal{P}_t^*(\ell, s, \text{SRC}, \text{LRC+1}), \\
&\qquad \ell, s, \text{SRC}, \text{LRC+1})] \\
&+ P_{c,rts} \cdot [\mathcal{E}_{rts} + \mathcal{E}_{cts\_tout} \\
&\qquad + \mathcal{E}(m^*(\ell, s, \text{SRC+1}, \text{LRC}), \mathcal{P}_t^*(\ell, s, \text{SRC+1}, \text{LRC}), \\
&\qquad \ell, s, \text{SRC+1}, \text{LRC})],
\end{aligned} \quad (4)$$

and

$$\begin{aligned}
&\mathcal{L}(m, \mathcal{P}_t, \ell, s, \text{SRC}, \text{LRC}) = \\
&(1 - P_{c,rts}) \cdot [1 - P_{e,data}(m, \mathcal{P}_t, \ell, s)] \cdot \ell \\
&+ (1 - P_{c,rts}) \cdot P_{e,data}(m, \mathcal{P}_t, \ell, s) \\
&\quad \cdot \mathcal{L}(m^*(\ell, s, \text{SRC}, \text{LRC+1}), \mathcal{P}_t^*(\ell, s, \text{SRC}, \text{LRC+1}), \\
&\qquad \ell, s, \text{SRC}, \text{LRC+1}) \\
&+ P_{c,rts} \cdot \mathcal{L}(m^*(\ell, s, \text{SRC+1}, \text{LRC}), \mathcal{P}_t^*(\ell, s, \text{SRC+1}, \text{LRC}), \\
&\qquad \ell, s, \text{SRC+1}, \text{LRC}),
\end{aligned} \quad (5)$$

respectively, where $P_{c,rts}$ is the RTS collision probability and varies with the network configuration, $P_{e,data}$, the data transmission error

probability, is a function of m, $\mathcal{P}_t$, ℓ, and s, and varies with the wireless channel noise model, and

$$\mathcal{E}_{rts-sifs-cts-sifs} = \mathcal{E}_{rts} + 2 \cdot \mathcal{E}_{sifs} + \mathcal{E}_{cts}. \quad (6)$$

Since an Ack (CTS) timeout is equal to a SIFS time, plus an Ack (CTS) transmission time, and plus a Slot time, we have

$$\mathcal{E}_{ack\_tout} = \mathcal{E}_{sifs} + \mathcal{E}_{ack} + \mathcal{E}_{slot}, \quad (7)$$

and

$$\mathcal{E}_{cts\_tout} = \mathcal{E}_{sifs} + \mathcal{E}_{cts} + \mathcal{E}_{slot}. \quad (8)$$

$\mathcal{E}_{rts}$, $\mathcal{E}_{data}$, $\mathcal{E}_{cts}$, and $\mathcal{E}_{ack}$ represent the energy consumed to transmit an RTS/Data frame, or receive a CTS/Ack frame, respectively. $\overline{\mathcal{E}}_{bkoff}$ and $\overline{\mathcal{E}}_{freeze}$ constitute the total energy consumption during a backoff period, and represent the energy consumption while the backoff counter is decrementing and the energy consumption while the backoff counter is frozen due to the busy medium, respectively. Moreover, $\mathcal{E}_{sifs}$, $\mathcal{E}_{difs}$, and $\mathcal{E}_{slot}$ denote the energy consumptions of a WLAN card being idle for SIFS time, DIFS time, and Slot time, respectively. Due to the space limitation, please refer to [12] for the details of the probability analysis and the energy consumption calculation.

Consequently, the best mode-power combination to transmit a data frame and the corresponding minimum average energy consumption are, respectively,

$$\begin{aligned}
&\{m^*(\ell, s, \text{SRC}, \text{LRC}), \mathcal{P}_t^*(\ell, s, \text{SRC}, \text{LRC})\} \\
&= \arg \min_{\{m, \mathcal{P}_t\}} \mathcal{J}(m, \mathcal{P}_t, \ell, s, \text{SRC}, \text{LRC}),
\end{aligned} \quad (9)$$

and

$$\begin{aligned}
\mathcal{J}^*(\ell, s, \text{SRC}, \text{LRC}) &= \mathcal{J}(m^*, \mathcal{P}_t^*, \ell, s, \text{SRC}, \text{LRC}) \\
&= \min_{\{m, \mathcal{P}_t\}} \mathcal{J}(m, \mathcal{P}_t, \ell, s, \text{SRC}, \text{LRC}).
\end{aligned} \quad (10)$$

Therefore, by using the special case as the boundary condition, we have fully specified the computation of the table entries of the mode-power combination table by Eqs. (1), (2), (3), (4), (5), and (9).

III. PERFORMANCE EVALUATION

In this section, we evaluate the effectiveness of our proposed energy-efficient DCF operation by simulation results. For simulation, we used the ns-2 simulator [13] and enhanced the original 802.11 DCF module provided by ns-2 to support 802.11a PHY, PHY rate adaptation, and TPC.

A. Simulation Setup

As specified in the 802.11 standard, the maximum transmit power is limited to 200 mW (i.e., 23 dBm) [4] for the middle band of the 5 GHz U-NII band, which is suitable for indoor environments. Therefore, in our simulation, a TPC-enabled 802.11a device is allowed to choose any one of the 15 transmit power levels (from -19 dBm to 23 dBm with 3 dBm gaps) to transmit a data frame, and 15 dBm is selected as the nominal transmit power by referring to the specification of the Agere ORiNOCO cards [14]. The background noise level is set to -93 dBm. Besides, we use a log-distance path loss model with path loss exponent of four [15] to simulate the

435

indoor office environment. The four testing schemes under consideration are:

- (I) RTS-CTS-Data(TPC)-Ack
- (II) RTS-CTS-Data(15dBm)-Ack
- (III) Data(TPC)-Ack
- (IV) Data(15dBm)-Ack

PHY rate adaptation is used in all testing schemes. Note that Scheme I is our proposed energy-efficient DCF operation. In order to have a fair comparison, the Ack and/or CTS frames are also transmitted using the full power in the other three testing schemes.

Each simulation run is performed for a duration of 10 seconds in an 802.11a infrastructure BSS with 8 wireless stations contending for uplink transmissions. Each station transmits in a greedy mode, i.e., its data queue is never empty. All the data frames are 1500-octet long and transmitted without fragmentation. The initial energy of each station is 1000 Joules, which is enough to keep stations operational without running out of energy during the simulation. Testing schemes are compared with each other in terms of the delivered data per unit of energy consumption (in MBits/Joule), which is calculated as the ratio of the total amount of uplink data received by the AP to the total energy consumption over all the wireless stations in the network. Note that the larger this value, the more energy-efficient a scheme is. We also compare the aggregate goodput (in Mbps) and the frame collision probability of the testing schemes.

B. The Mode-Power Combination Table

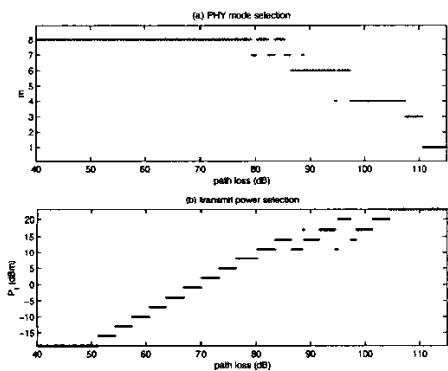Fig. 3 shows a snapshot of the (4-dimensional) mode-power combination table when $\ell = 1500$ and (SRC, LRC) = (0, 0).

Fig. 3. A snapshot of the mode-power combination table when $\ell = 1500$ and (SRC, LRC) = (0, 0)

We have three observations. First, when the path loss is large, the lower PHY modes are preferred since they are more robust and have better error performance. On the other hand, when the path loss is small, higher PHY modes are used to save energy since the duration of a single transmission attempt is shorter. Second, a low transmit power level does not necessarily result in low energy consumption. This is because, for the same PHY mode, adopting a lower transmit power level may lead to less energy consumption in one single transmission attempt, but the consequent low signal-to-noise ratio at the receiver side may cause more re-transmissions and hence greater total energy consumption. Third, the combination of a higher PHY mode with stronger transmit power may result in lower energy consumption than the combination of a lower PHY

mode with rather weaker transmit power. For example, as shown in the figure, when the path loss is about 80 dB, PHY mode 7 is selected with the transmit power of 8 dBm, while for the path loss slightly higher than 80 dB, PHY mode 8 is used again, however, with a higher power level at 11 dBm. Similar switch-backs can also be observed at other path loss ranges in the figure.

The snapshots for other ℓ, SRC, and LRC values can be approximately viewed as different shifted versions of Fig. 3. In general, when a data frame carries a larger payload ($\ell\uparrow$) or less transmission attempts remain for a data frame (SRC$\uparrow$ and/or LRC$\uparrow$), the figure shifts left and the more conservative combinations (i.e., lower PHY mode and higher transmit power) are selected under the same path loss condition; otherwise, it shifts right.

C. Simulation Results

We first compare the testing schemes in the star-topology wireless networks, where 8 wireless stations are evenly spaced on a circle centered by the AP with the radius of r. In the simulation, we set the carrier sensing threshold to -91 dBm, meaning that if the distance between two wireless stations results in a path loss larger than $(\mathcal{P}_t+91)$ dB, the two stations are hidden to each other. Clearly, the hidden node ratio (δ) of a star-topology wireless network varies with different transmit power levels and different network sizes. We evaluate the performance of the testing schemes for 5 different network sizes, and Table I lists the r values and the corresponding hidden node ratios for nominal transmit power.

TABLE I
HIDDEN NODE RATIOS OF DIFFERENT STAR-TOPOLOGY NETWORKS

r (m)	1	12	15	20	28
δ	0	0	1/7	3/7	5/7

The comparison results of the delivered data per Joule, the aggregate goodput, and the frame collision probability are shown in Figs. 4(a), (b), and (c), respectively. The "random" topology shown as the last columns in the figure will be discussed later. We have the following three main observations.

First, Scheme I consistently outperforms Scheme II in terms of the delivered data per Joule in all the simulated networks. This is reasonable because Scheme I is designed to be the most energy-efficient in transmitting data frames via four-way handshakes. For example, when $r = 1$ or 12, although Scheme I and II achieve comparable aggregate goodput since they use the same PHY mode, Scheme I transmits data frames using a power level lower than 15 dBm to save energy. Besides, it is interesting to notice that, when a = 28, Scheme II shows very low aggregate goodput. This is because even with the most robust PHY mode, the fixed 15 dBm transmit power used in Scheme II is still not high enough to combat the very high path loss, thus resulting in a significant number of data transmission errors.

Second, when there are no hidden terminals in the network ($r = 1$ or 12), all four schemes present similar frame collision probabilities, and Scheme I results in a lower aggregate goodput than Schemes III and IV due to the additional RTS/CTS frame exchanges before the data transmissions. When the path loss is very small ($r = 1$), Scheme I is able to select a very low power level for its data transmissions. As a result, Scheme I and IV shows comparable energy-efficiency performances, which is evidenced by similar

436

(a) delivered data per Joule (b) aggregate goodput (c) frame collision probability
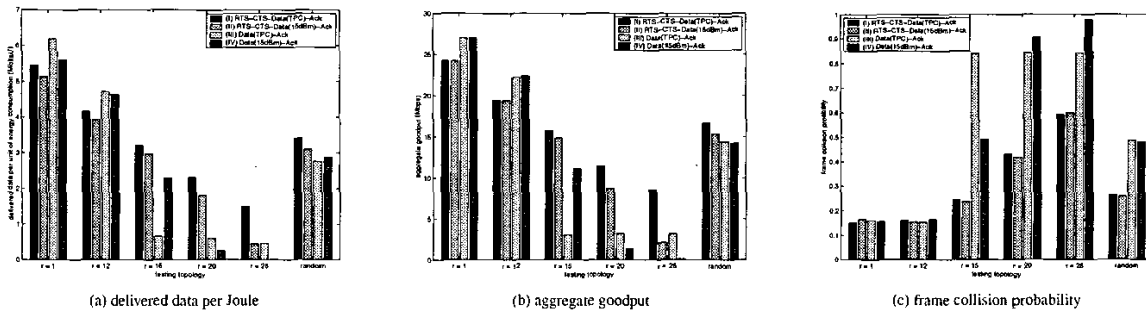
Fig. 4. Comparison of the testing schemes

values of the delivered data per Joule. However, when the path loss is large ($r = 12$), Scheme I has to select a high power level for its data transmissions and, in turn, shows worse energy-efficiency performance than both Schemes III and IV. Actually, this is the worst scenario for our proposed scheme.

Third, when there are hidden terminals in the network ($r = 15, 20$, or 28), the performance of all four schemes degrades. With a larger hidden node ratio, more stations are hidden to each other in the network and the frame collision probability increases, thus the performance degrades even more. Schemes I and II are less affected by the presence of hidden terminals than Schemes III and IV because, by exchanging the RTS/CTS frames to reserve the wireless medium before the actual data transmission, the collisions can only occur to the RTS frames whose transmission time is much shorter than that of the data frames. As mentioned in Section I, one potential problem of applying TPC directly to the data transmissions is that it might result in more hidden terminals. We observe such problem in the simulated network of $r = 15$. In this case, Scheme III selects the mode-power combination of PHY mode 4 and 11 dBm for the data transmissions, while all the other schemes use the nominal 15 dBm power level to attempt either RTS or data transmissions to contend for the wireless medium. As a result, the hidden node ratio of the network, when Scheme III is used, becomes 3/7 instead of 1/7. On the other hand, in the simulated network of $r = 28$, Scheme III selects the mode-power combination of PHY mode 4 and 23 dBm, which actually results in less hidden terminals ($\delta = 3/7$). The facts explained above are supported by the similar frame collision probabilities for Scheme III when $r = 15$, 20, and 28. Note that when $r = 20$, Scheme III selects the mode-power combination of PHY mode 4 and 17 dBm. Another observation is the extremely small values of the delivered data per Joule and the aggregate goodput when Scheme IV is used in the simulated network of $r = 28$. This is because Scheme IV suffers both a high frame collision probability — which is due to the large hidden node ratio and the long data transmission time — and a high data transmission error probability due to the large path loss.

We also evaluate the performances of the testing schemes in randomly-generated network topologies: the initial locations of the 8 wireless stations in the network are arbitrarily determined, and each station can move in any direction with speed up to 5m/s — which is considered as the maximum speed for indoor movements. The results are averaged over 10 different random topologies and shown as the last columns in Figs. 4(a), (b), and (c). Clearly, our proposed scheme performs the best.

IV. CONCLUSION

In this paper, we demonstrate the energy-efficient DCF operation via TPC and PHY rate adaptation in IEEE 802.11a infrastructure BSSs. The key idea is to enforce the RTS/CTS frame exchange before each data transmission, and then select the most energy-efficient mode-power combination for the subsequent data frame transmission. We compare the energy-efficiency and aggregate-goodput performances of the proposed scheme against three other schemes: RTS-CTS-Data(15dBm)-Ack, Data(TPC)-Ack, and Data(15dBm)-Ack. Simulation results show that our scheme consistently outperforms the RTS-CTS-Data(15dBm)-Ack scheme and is significantly better than the Data(TPC/15dBm)-Ack schemes in the presence of hidden terminals — which are often found in the real networks.

REFERENCES

[1] IEEE 802.11, *Part 11: Wireless LAN Medium Access Control (MAC) and Physical Layer (PHY) Specifications.* IEEE, Aug. 1999.

[2] IEEE 802.11a, *Part 11: Wireless LAN Medium Access Control (MAC) and Physical Layer (PHY) Specifications: High-speed Physical Layer in the 5 GHz Band.* Supplement to IEEE 802.11 Standard, Sep. 1999.

[3] Daji Qiao, Sunghyun Choi, Amjad Soomro, and Kang G. Shin. "Energy-Efficient PCF Operation of IEEE 802.11a Wireless LAN," in *Proc. IEEE INFOCOM'02*, New York City, NY, Jun. 2002, vol. 2, pp. 580–589.

[4] Bob O'Hara and Al Petrick, *The IEEE 802.11 Handbook: A Designer's Companion*, Standards Information Network, IEEE Press, 1999.

[5] Steven D. Gray and Venkatesh Vadde, "Throughput and Loss Packet Performance of DCF with Variable Transmit Power." IEEE 802.11-01/227, May 2001.

[6] Tajana Simunic, Luca Benini, Peter Glynn, and Giovanni De Micheli, "Dynamic Power Management for Portable Systems," in *Proc. ACM MobiCom'00*, Boston, MA, Aug. 2000, pp. 11–19.

[7] Mark Stemm, Paul Gauthier, Daishi Harada, and Randy H. Katz. "Reducing Power Consumption of Network Interfaces in Hand-Held Devices," in *Proc. 3rd International Workshop on Mobile Multimedia Communications*, Princeton, NJ, Sep. 1996.

[8] Eun-Sun Jung and Nitin H. Vaidya, "An Energy Efficient MAC Protocol for Wireless LANs," in *Proc. IEEE INFOCOM'02*, New York City, NY, Jun. 2002, vol. 3, pp. 1756–1764.

[9] Javier Gomez, Andrew T. Campbell, Mahmoud Naghshineh, and Chatschik Bisdikian, "Conserving Transmission Power in Wireless Ad Hoc Networks," in *Proc. IEEE ICNP'01*, Nov. 2001, pp. 24–34.

[10] Sharad Agarwal, Srikanth V. Krishnamurthy, Randy K. Katz, and Son K. Dao. "Distributed Power Control in Ad-Hoc Wireless Networks," in *Proc. IEEE PIMRC'01*, 2001, pp. 59–66.

[11] Jean-Pierre Ebert and Adam Wolisz. "Combined Tuning of RF Power and Medium Access Control for WLANs," *Mobile Networks & Applications*, vol. 5, no. 6, pp. 417–426, Sep. 2001.

[12] Daji Qiao, Sunghyun Choi, Amit Jain, and Kang G. Shin. "Energy-Efficient DCF Operation of IEEE 802.11a Wireless LAN," Tech. Rep., The University of Michigan, Ann Arbor, MI, Aug. 2002.

[13] "The Network Simulator – ns-2," http://www.isi.edu/nsnam/ns/. Online Link.

[14] Agere Systems. *User's Guide for ORiNOCO PC Card*, Sep. 2000.

[15] T. S. Rappaport, *Wireless Communications: Principle and Practice*, Englewood Cliffs, NJ: Prentice-Hall, 1996.